BAAA, Vol. 63, 2022
R.D. Rohrmann, M.N. Gómez, C.E. Boeris & M.A. Sgró, eds.

Asociación Argentina de Astronomía
Boletín de artículos científicos

Colliding winds in ultraluminous X-ray sources

L. Abaroa[1,2], G.E. Romero[1,2] & P. Sotomayor Checa[1,2]

[1] *Facultad de Ciencias Astronómicas y Geofísicas, UNLP, Argentina*
[2] *Instituto Argentino de Radioastronomía, CONICET–CICPBA–UNLP, Argentina*

Contact / leandroabaroa@gmail.com

Resumen / Las fuentes ultraluminosas de rayos X (ULX) son objetos con luminosidades que superan el límite de Eddington para un agujero negro de masa estelar. En estos sistemas binarios cerrados, la estrella desborda su lóbulo de Roche y el agujero negro acreta materia a tasas súper críticas. Las capas superiores del disco dejan de estar en equilibrio y son expulsadas en forma de un viento poderoso impulsado por la radiación, que interactúa con el viento de la estrella compañera produciendo choques donde las partículas pueden ser aceleradas hasta energías relativistas para luego enfriarse exhibiendo un amplio espectro.

Abstract / Ultraluminous X-ray sources (ULX) are objects with luminosities that exceed the Eddington limit for a stellar-mass black hole. In these closed binary systems, the star overflows its Roche lobe and the black hole accretes matter at a supercritical rate. The upper layers of the disk are no longer in equilibrium and are ejected as a powerful radiation-driven wind that interacts with the wind from the star producing shocks where particles can be accelerated up to relativistic energies and then cool down yielding a broadband spectrum.

Keywords / accretion, accretion disks — radiation mechanisms: non-thermal — stars: black holes — stars: winds, outflows — X-rays: binaries

1. Introduction

ULXs are point-like objects where the luminosity in the X-ray band is higher than the Eddington luminosity ($\sim 10^{39}$erg s^{-1} for a black hole of $\sim 10 M_\odot$). In these binary systems, a star and a compact object are gravitational linked. The star fills its Roche Lobe and transfers mass to the compact object through the Lagrange point. An accretion disk is formed because of the angular momentum in the system. In its inner region, the disk can have temperatures of several 10^7K. Because of the strong radiation fields, the disk surface is no longer in equilibrium and radiatively-driven particles are ejected, reaching semi-relativistic velocities. This disk-driven wind should interact with the stellar wind, where shocks are generated and particles can be accelerated, cooling down and producing non-thermal emission.

In this work we model the accretion disk and its wind, using a gravitational pseudo-potential. Then, we study the collision of winds and calculate the non-thermal radiation in a ULX with typical parameters.

2. The model

The ULX of our model is composed by a stellar-mass black hole (BH), and a Population I star (PopI star), with an orbital semi-axis of $a_0 = 5.8 R_\odot$.

Hereafter, $r_g = GM_{BH}/c^2$ is the gravitational radius of the BH, with G the gravitational constant, M_{BH} the BH-mass, and c the speed of light.

In the following, we describe the star and the semi-analytical models we use to study the BH, the accretion disk, and the disk-driven wind.

Star: Wolf-Rayet (WR) stars have powerful, line-driven winds. We assume in this model that the binary system has a star whose parameters are detailed in Table 1, which are based in typical values found in the literature (see eg., Sander et al., 2012).

WR Star		
Parameter	Value	Unity
M_*	17	$M_\odot$
R_*	3	$R_\odot$
$T_{\rm eff}$	79×10^3	K
$\dot{M}_*$	3.4×10^{-5}	$M_\odot$ yr^{-1}
$v_{*\rm w}$	1400	km s^{-1}
$v_{\rm rot}$	500	km s^{-1}
B_*	100	G

Table 1: Parameters of the WR-star adopted in this model. $v_{*\rm w}$ is the wind-velocity, $v_{\rm rot}$ the rotational speed, B_* is the magnetic field, and $\dot{M}_*$ the mass-loss rate.

Black hole: we mimic the effects of general relativity in the vicinity of the BH using the gravitational pseudo-potential given by Artemova et al. (1996); Aktar et al. (2019):

$$\Phi_g = \begin{cases} \frac{GM_{BH}}{(\beta-1)r_H}\left[1 - \left(\frac{r}{r-r_H}\right)^{\beta-1}\right], & \beta \neq 1 \\ \frac{GM_{BH}}{r_H}\ln\left(1-\frac{r_H}{r}\right), & \beta = 1 \end{cases} \quad (1)$$

with $\beta = r_{in}/r_H - 1$. Here, $r_{in}(a)$ is the inner radius of the accretion disk, and $r_H(a)$ the radius of the event horizon (see Bardeen et al., 1972). $0 \leq a \leq 1$ is the spin

Oral contribution

parameter of the BH. We consider a non-rotating BH with a mass of $13M_\odot$:

$a = 0 \rightarrow r_{\rm H} = 2r_{\rm g},\ r_{\rm in} = 6r_{\rm g} \rightarrow \beta = 2.$

Accretion disk: the critical mass-accretion rate in the disk is given by $\dot{M}_{\rm crit} = L_{\rm Edd}/c^2$, with $L_{\rm Edd}$ the Eddington luminosity (Fukue, 2004). We adopt a non-magnetized, standard-like disk model with a super-critical accretion rate ($\dot{M}_{\rm acc} = 12\dot{M}_{\rm crit}$), where the viscous heating is balanced with the radiative cooling, $Q_{\rm vis} = Q_{\rm rad}$. We use cylindrical coordinates (r, ϕ, z), and neglect the self-gravity of the disk gas. Since the disk is optically-thick, we assume that it radiates as a blackbody.

The intensity of the disk radiation at any point above or below the disk, at a radius $r_{\rm d}$, is given by:

$$I = \frac{3GM_{\rm BH}\dot{M}_{\rm acc}}{8\pi^2 r_{\rm d}^3} D^4 g f, \tag{2}$$

where $D = (1+z_{\rm red})^{-1}$ is the relativistic Doppler factor, and $z_{\rm red}$ is the redshift factor (see Hirai & Fukue, 2001, for the expressions of the correction factors g and f).

We obtain the spatial distribution of the radiation fields by calculating the energy-momentum tensor (Rybicki & Lightman, 1986):

$$R^{\mu\nu} = \begin{pmatrix} E & \frac{1}{c}F^\alpha \\ \frac{1}{c}F^\alpha & P^{\alpha\beta} \end{pmatrix} = \frac{1}{c}\int I j^\mu j^\nu {\rm d}\Omega, \tag{3}$$

where E is the energy-density, F^α the flux vector, and $P^{\alpha\beta}$ the pressure-tensor. I is the intensity from Eq. 2, j is the cosine director and Ω the solid angle. Our treatment includes radiation drag and ignores the light-bending effect.

Wind: the wind ejected from the accretion disk is radiatively-driven. We follow a particle-treatment to calculate the velocity and trajectory of the ionized wind.

We solve the total tensorial-differential equation in order to find the velocity and trajectory of the wind-particles (Hirai & Fukue, 2001):

$$\begin{aligned} c\frac{du^\alpha}{d\tau} = &- \frac{\partial \Phi_{\rm eff}}{\partial x^\alpha} + \\ &+ \frac{\sigma_T}{mc}[\gamma F^\alpha - cP^{\alpha\beta}u_\beta - c\gamma^2 E u^\alpha + \\ &+ cu^\alpha(\frac{2\gamma}{c}F^\beta u^\beta - P^{\beta\gamma}u_\beta u_\gamma)], \end{aligned} \tag{4}$$

where u^α denotes the four-velocity of the wind-particles, m is the particle mass, σ_T is the Thomson-scattering cross section, and γ the Lorentz factor.

As initial condition we assume that the gas particles corotate with the disk at the launching radius, $u_0^\alpha = (0, l_0/r_0, 0)$, with l the angular momentum per unit mass.

3. Winds collision

3.1. Contact discontinuity and magnetic field

The winds of the disk and the star collide at a surface called contact-discontinuity (CD) that separates the shocked and the unshocked regions. The apex of the bow-shock is located where the ram pressures of the winds are in equilibrium: $P_{\rm ram}(r_{\rm BH}) = \rho_{\rm dw}v_{\rm dw}^2 = \rho_{*\rm w}v_{*\rm w}^2 = P_{\rm ram}(r_{\rm S})$, with ρ the density and v the velocity. Here, $r_{\rm BH}$ and $r_{\rm S}$ are the distances to the CD, from the BH and the stellar center, respectively. We obtain $r_{\rm S} \approx R_*$; hence, the stellar wind is unable of halting the wind of the disk.

The width of the acceleration region, $\Delta x_{\rm ac}$, depends on the cooling-length, the location of the CD, and the Larmor radius of the particles. Since we adopt a one-zone model, the acceleration region is narrow enough to generate near-homogeneity conditions.

Since $r_{\rm S} \approx R_*$, the magnetic field at the CD is $B_{\rm CD} \approx B_*$.

3.2. Particle acceleration and radiative processes

Particles are accelerated in the collision region through first-order diffusive shock mechanism. A small fraction of the total kinetic power of the wind is transferred to relativistic particles, $L_{\rm rel} = 0.1L_{\rm K}$ ($L_{\rm K} = \dot{M}v^2/2$), where we assume equipartition between relativistic protons and electrons. The shock propagates perpendicular to the magnetic field, with a Bohm-diffusion coefficient. The pressure and density in the shocked medium are calculated following the Rankine-Hugoniot relations (Lamers & Cassinelli, 1999).

The shock is adiabatic if the thermal cooling-length R_Λ is longer than the width of the acceleration region (see McCray & Snow, 1979; Wolfire et al., 2003). In our model we obtain $R_\Lambda \approx 10^{13}{\rm cm} \gg 10^{10}{\rm cm} \approx \Delta x_{\rm ac}$; therefore, the adiabaticity condition is fullfiled.

Particles accelerated at the shock can cool through adiabatic and radiative processes. The adiabatic cooling is related to the work done by the particles of the wind to expand the shocked gas. The radiative cooling is caused by the interaction of particles with ambient fields and cold matter. We adopt a lepto-hadronic model, and calculate numerically the following radiative processes: synchrotron, inverse Compton (IC), Bremmstrahlung, photo-hadronic interactions, and proton-proton collisions (see eg., Romero & Paredes, 2011).

In order to obtain the particle-distribution, we solve numerically the transport equation in steady state in the one-zone region. The convection time only depends on the macroscopic velocity of the fluid, and the space-scale of the problem.

We calculate the spectral energy distribution (SED) by obtaining the luminosity per unit of energy as a function of the energy of the photon, for each of the relevant processes involved in the cooling. Finally we calculate the absorption by pair creation from photon-photon annihilation, $\gamma + \gamma \rightarrow e^+ + e^-$. The non-thermal photons in the acceleration region are the projectiles, and the targets are the photons of the radiation field provided by the star.

4. Results

4.1. Wind velocity and trajectory

We solve numerically Eq. 4 and find the velocity and trajectory of the particles in the wind of the disk. As

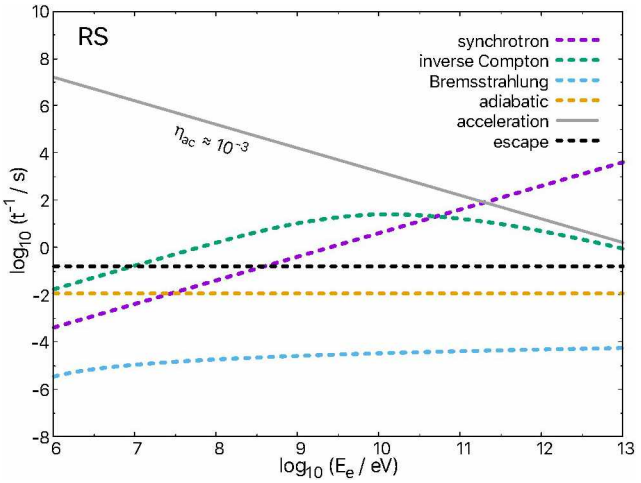

Figure 1: Time-scales in logarithmic scale of the electron acceleration, escape and cooling. The acceleration efficiency is $\sim 10^{-3}$, and the maximum energy reached by the electrons is ~ 500 GeV.

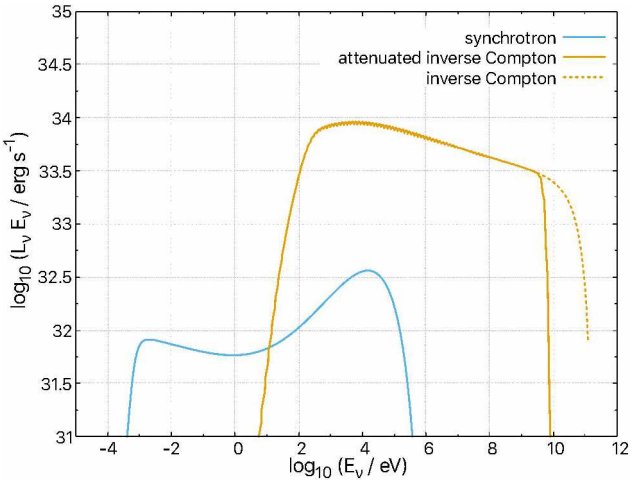

Figure 2: Non-thermal spectral energy distributions in logarithmic scale for the synchrotron and inverse Compton processes. The dotted line is the non-attenuated IC spectrum. There is a maximum of the emission at $E \approx 10$ keV.

initial conditions, we set the normalized accretion rate at $\dot{m} = 12$ (in units of $\dot{M}_{\rm crit}$), and the launching radius for the wind at $r_0 = 10\ r_{\rm g}$. The particle trajectory is helical for $r < 20 r_{\rm g}$ and then the particles follow a free path. The terminal velocity obtained is $\sim 0.12c$.

The semi relativistic radiatively-driven wind of the disk suppresses the wind of the star, colliding with the stellar surface. A reverse shock (RS) is formed.

4.2. Time scales and particle distribution

Fig. 1 shows the energy gain and losses of the particles in the RS. We consider only the electrons, since protons escape from the acceleration region without cooling. The acceleration efficiency of the process is $\eta_{\rm ac} \approx 10^{-3}$ ($\propto v_{\rm sh}^2/c^2$, $v_{\rm sh}$ the shock velocity).

The electrons cool through IC and synchrotron mechanisms. IC dominates between energies of ~ 10 MeV $- 10$ GeV. Electrons with energies $E < 10$ MeV escape from the acceleration region without cooling. The maximum energy reached by the particles is ~ 500 GeV. Highly-relativistic protons (with energies $E > 100$ TeV) are injected in the interstellar medium.

We solve the transport equation for the electrons considering only IC and synchrotron losses, and a power-law injection function with a spectral index 2.2 and an exponential cutoff.

4.3. Spectral energy distribution

The ULX yields a wide spectrum. In the radio band the luminosity is $\sim 10^{32}$ erg s^{-1}, while in X-rays and gamma-rays reaches $\sim 10^{34}$ erg s^{-1} (Fig. 2). The attenuation factor has effect on the luminosity for energies > 10 GeV. We plot in Fig. 2 the non-thermal contributions in the system, considering the absorption.

5. Conclusions

We have modeled a ULX where a super-critical accretion disk launches winds. This wind collides with the wind of the PopI star. This interaction allows the formation of a reverse shock causing the acceleration of particles up to relativistic energies. Non-thermal high energy emission is produced via IC scattering.

We conclude that the interaction between the radiatively-driven winds of the accretion disk and the wind of companion star is able to produce hard X-rays and gamma rays in some ULXs.

Acknowledgements: The authors are very grateful to Dr. Daniela Pérez for her collaboration and useful discussion. G.E.R. acknowledges support from the Spanish Ministerio de Ciencia e Innovación under grant PID2019-105510GB-C31 and through the "Center of Excellence María de Maeztu 2020-2023" award to the ICCUB (CEX2019-000918-M).

References

Aktar R., Nandi A., Das S., 2019, Ap&SS, 364, 22
Artemova I.V., Bjoernsson G., Novikov I.D., 1996, ApJ, 461, 565
Bardeen J.M., Press W.H., Teukolsky S.A., 1972, ApJ, 178, 347
Fukue J., 2004, PASJ, 56, 569
Hirai Y., Fukue J., 2001, PASJ, 53, 285
Lamers H.J.G.L.M., Cassinelli J.P., 1999, *Introduction to Stellar Winds. Cambridge: Cambridge University Press.*
McCray R., Snow T. P. J., 1979, ARA&A, 17, 213
Romero G.E., Paredes J.M., 2011, *Introducción a la Astrofísica Relativista. Barcelona: Universitat de Barcelona.*
Rybicki G.B., Lightman A.P., 1986, *Radiative Processes in Astrophysics. New York: Wiley VCH.*
Sander A., Hamann W.R., Todt H., 2012, A&A, 540, A144
Wolfire M.G., et al., 2003, ApJ, 587, 278